

## Supplementary Information

### Copper nanocrystals anchored on O-riched carbonized corn gel for nitrogen electroreduction to ammonia

Chang Li,<sup>a,b,‡</sup> Shengbo Zhang,<sup>a,b,‡</sup> Zhenhua Ding,<sup>c</sup> Hongjian Zhou,<sup>\*,a</sup>

Guozhong Wang,<sup>a</sup> Haimin Zhang,<sup>\*,a</sup>

<sup>a</sup> Key Laboratory of Materials Physics, Centre for Environmental and Energy Nanomaterials, Anhui Key Laboratory of Nanomaterials and Nanotechnology, CAS Center for Excellence in Nanoscience, Institute of Solid State Physics, Chinese Academy of Sciences, Hefei 230031, China.

<sup>b</sup> University of Science and Technology of China, Hefei 230026, China.

<sup>c</sup> Anhui Institute of Product Quality Supervision and Inspection, Hefei 230051, China.

<sup>‡</sup> These authors contributed equally to this work.

\* Corresponding authors: [hjzhou@issp.ac.cn](mailto:hjzhou@issp.ac.cn) (H. Zhou); [zhanghm@issp.ac.cn](mailto:zhanghm@issp.ac.cn) (H. Zhang).

### Experimental Section

#### *Materials and Reagents:*

The corn gel (CG) was provided by the Anhui Institute of Product Quality Supervision and Inspection, China. Copper sulfate ( $\text{CuSO}_4 \cdot 5\text{H}_2\text{O}$ ) were purchased from Sinopharm Chemical Reagent Co., Ltd. All of the chemical reagents were analytical grade and were used without further purification.

#### *Synthesis of Cu NCs/CCG:*

First, the corn gel was immersed in a 400 mL aqueous solution containing 40 mmol  $\text{CuSO}_4 \cdot 5\text{H}_2\text{O}$  for 8 hours. After the adsorption of  $\text{Cu}^{2+}$ , the corn gel was freeze-dried and subjected to pyrolysis at 400 °C for 2 h, and then carbonized at 700 °C for 3 h in Ar atmosphere to obtain a metal Cu nanoparticles anchored on corn gel derived graphitic carbon substrate (Cu NPs/CCG). Subsequently, the obtained Cu NPs/CCG

was dried at 80 °C under a vacuum condition for 8 hours, and then subjected to acid etching treatment using 9.2 M H<sub>2</sub>SO<sub>4</sub> at a temperature of 120 °C for 6 hours to remove metallic Cu NPs. The obtained Cu nanocrystals anchored carbonized corn gels (Cu NCs/CCG) after acid etching were dried at 80 °C under a vacuum condition for 10 hours. For comparison, carbonized corn gels (CCG) was obtained from carbonization of corn gels as the same fabrication procedure as Cu NPs/CCG except for no addition of CuSO<sub>4</sub>·5H<sub>2</sub>O.

### ***Characterizations:***

The Fourier transform infrared (FT-IR) spectrum of samples were measured on a Nicolet-Nexus FT-IR spectrometer with the KBr pellet technique ranging from 400 to 4000 cm<sup>-1</sup> at room temperature. Raman spectra were recorded by Renishaw Micro-Raman Spectroscopy (Renishaw inVia Reflex) with 532 nm laser excitation. The crystalline structures of samples were identified by X-ray diffraction analysis (XRD, Philip X'pert PRO) using Nifiltered monochromatic CuK $\alpha$ 1 radiation ( $\lambda$ K $\alpha$ 1 = 1.5418 Å) at 40 kV and 40 mA. The morphologies of materials were characterized by Scanning electron microscopy (SEM, SU 8020) at an acceleration voltage of 5.0 kV, and High-resolution transmission electron microscope (HRTEM, JEMARM 200F) at an accelerating voltage of 200 kV. X-ray photoelectron spectroscopy (XPS) analysis was performed on an ESCALAB 250 X-ray photoelectron spectrometer (Thermo, America) equipped with Al K $\alpha$ 1, monochromatized radiations at 1486.6 eV Xray source. The Cu L-edge NEXAFS soft X-ray absorption spectroscopy (sXAS) spectra were measured at the photoemission end-station at beamline BL10B in the National Synchrotron Radiation Laboratory (NSRL) in Hefei, China. A bending magnet was connected to the beamline, which is equipped with three gratings covering photon energies from 100 to 1000 eV. In this experiment, the samples were kept in the total electron yield mode under an ultrahigh vacuum at 5×10<sup>-10</sup> mbar. The resolving power of the grating was typically E/ $\Delta$ E = 1000, and the photon flux was 1 ×10<sup>10</sup> photons per s. Spectra were collected at energies from 100 to 1000 eV in 0.2 eV energy steps. The NEXAFS raw data were normalized by a procedure consisting of several steps.

First, the photon energy was calibrated from the 4f spectral peak of a freshly sputtered gold wafer. Then substrate a line to set the pre-edge to be zero. Finally, the spectra were normalized to yield an edge-jump to one.

### ***Electrochemical measurements:***

Electrochemical measurements were performed on an electrochemical workstation (CHI 660E, CH Instruments, Inc., Shanghai, China). All electrochemical measurements were performed on a CHI 660E electrochemical workstation (CH Instrumental Corporation, Shanghai, China) using a two-compartment cell, which was separated by Nafion 117 proton exchange membrane. Different catalyst inks were prepared by dispersing 5 mg sample into 100  $\mu\text{L}$  of ethanol and 5.0  $\mu\text{L}$  of Nafion (5 wt.%) under ultrasonic, and were then dropped on carbon cloth with  $1 \times 1 \text{ cm}^2$  for fabrication of the working electrode. Ag/AgCl electrode and Pt net were used as reference electrode and counter electrode, respectively. The polarization curves were measured with a scan rate of  $5.0 \text{ mV s}^{-1}$  at room temperature and all polarization curves were obtained at the steady-state ones after several cycles. For electrochemical  $\text{N}_2$  reduction reaction (ENRR) experiments, the potentiostatic test was conducted for 2 h in  $\text{N}_2$ -saturated 0.1 M  $\text{Na}_2\text{SO}_4$  solution (30 mL, pH=5.9) by continuously supplying  $\text{N}_2$  into the electrolyte under ambient conditions. Prior to ENRR measurements,  $\text{N}_2$  feeding gas was first purged through a 1.0 mM  $\text{H}_2\text{SO}_4$  solution and distilled water to eliminate the potential  $\text{NO}_x$  and  $\text{NH}_3$  contaminants. In this work, all measured potentials (vs. Ag/AgCl) were transformed into the potentials vs. reversible hydrogen electrode (RHE) based on the following equation:

$$E_{\text{RHE}} = E_{\text{Ag/AgCl}} + 0.059\text{pH} + E^{\circ}_{\text{Ag/AgCl}}$$

### ***Determination of ammonia:***

Concentration of the produced ammonia was spectrophotometrically detected by the indophenol blue method. In detail, 2.0 mL of sample was taken, and then diluted with 8.0 mL of deionized water. Subsequently, 100  $\mu\text{L}$  of oxidizing solution (sodium hypochlorite ( $\rho\text{Cl}=4\sim 4.9$ ) and 0.75 M sodium hydroxide), 500  $\mu\text{L}$  of colouring solution (0.4 M sodium salicylate and 0.32 M sodium hydroxide) and 100  $\mu\text{L}$  of

catalyst solution (0.1g Na<sub>2</sub>[Fe(CN)<sub>5</sub>NO]·2H<sub>2</sub>O diluted to 10 mL with deionized water) were added to the measured sample solution, respectively. After the placement of 1 h at room temperature, the absorbance measurements were performed at wavelength of 697.5 nm. The obtained calibration curve was used to calculate the ammonia concentration in the samples.

***Determination of hydrazine :***

The hydrazine present in the electrolyte was estimated by the method of Watt and Chrisp. A mixture of para-(dimethylamino) benzaldehyde (5.99 g), HCl (concentrated, 30 mL) and ethanol (300 mL) was used as a color reagent. In detail, 2 mL of sample was taken, and then diluted with 8 mL HCl solution (0.1 M). Subsequently, 5.0 mL of the as-prepared color reagent was added to the above sample solution. Finally, the absorbance measurements were performed after the placement of 20 min at wavelength of 455 nm. The obtained calibration curve was used to calculate the N<sub>2</sub>H<sub>4</sub>·H<sub>2</sub>O concentration.

***Calculations of NH<sub>3</sub> yield rate (R(NH<sub>3</sub>)) and Faradaic efficiency (FE(NH<sub>3</sub>)):***

$$R(NH_3)(\mu g h^{-1} mg^{-1}_{cat}) = \frac{C(NH_3)(\mu g mL^{-1}) \times V(mL)}{t(h) \times m(mg)}$$

Where, C<sub>NH<sub>3</sub></sub> and V are the measured NH<sub>3</sub> concentration and the electrolyte solution volume, respectively, t is the ENRR reaction period and m. is the amount of the loaded catalyst.

$$FE(NH_3)(\%) = \frac{3 \times n(NH_3)(mol) \times F}{Q} \times 100\%$$

Where F is the Faradaic constant (96485.34); Q is the total charge transferred during the ENRR.

## Supplementary Tables and Figures

**Table S1.** The comparison of our work and other recently reported ENRR electrocatalysts.

Catalyst	System /Conditions	NH <sub>3</sub> Production Rate ( $\mu\text{g h}^{-1} \text{mg}^{-1}$ )	FE (%)	Ref.
<b>Cu NCs/CCG</b>	<b>0.1M Na<sub>2</sub>SO<sub>4</sub></b>	<b>1514 <math>\mu\text{g h}^{-1} \text{mg}_{\text{Cu}}^{-1}</math></b> <b>(-0.3 V vs. RHE)</b>	<b>25.89</b>	<b>This work</b>
Cu-CeO <sub>2</sub> -3.9	0.1 M Na <sub>2</sub> SO <sub>4</sub> (pH = 6.3)	8.109 $\mu\text{g h}^{-1} \text{mg}^{-1}$ (-0.1 V vs. RHE)	19.1	1
CuO/RGO	0.1 M Na <sub>2</sub> SO <sub>4</sub>	3.15 $\mu\text{g h}^{-1} \text{mg}_{\text{cat}}^{-1}$ (-0.75 V vs. RHE)	3.9	2
Cu/AC-S	0.1 M Na <sub>2</sub> SO <sub>4</sub> (pH = 6.3)	9.7 $\mu\text{g h}^{-1} \text{mg}_{\text{cat}}^{-1}$ (-0.3 V vs. RHE)	15.9	3
Cu/PI-300	0.1 M KOH	3.44 $\mu\text{g h}^{-1} \text{mg}_{\text{cat}}^{-1}$ (-0.4 V vs. RHE)	6.56	4
Cu SAC	0.1 M KOH	$\sim 53.3 \mu\text{g h}^{-1} \text{mg}_{\text{cat}}^{-1}$ (-0.35 V vs. RHE)	13.8	5
Cu NPs-rGO	0.5 M LiClO <sub>4</sub>	24.58 $\mu\text{g h}^{-1} \text{mg}_{\text{cat}}^{-1}$ (-0.4 V vs. RHE)	15.32	6
Ag <sub>3</sub> Cu BPNs	0.1 M Na <sub>2</sub> SO <sub>4</sub>	24.59 $\mu\text{g h}^{-1} \text{mg}_{\text{cat}}^{-1}$ (-0.5 V vs. RHE)	13.28	7
BCC PdCu	0.5 M LiCl	35.7 $\mu\text{g h}^{-1} \text{mg}_{\text{cat}}^{-1}$ (-0.1 V vs. RHE)	11.5	8
Au /TiO <sub>2</sub>	0.1 M HCl	21.4 $\mu\text{g h}^{-1} \text{mg}_{\text{cat}}^{-1}$ (-0.2 V vs. RHE)	8.11	9
Au nanorods	0.1 M KOH	1.648 $\mu\text{g h}^{-1} \text{mg}_{\text{cat}}^{-1}$ N <sub>2</sub> H <sub>4</sub> H <sub>2</sub> O: 0.102 $\mu\text{g h}^{-1} \text{mg}_{\text{cat}}^{-1}$ (-0.2 V vs. RHE)	3.87	10
Ru SAs/N-C	0.05 M H <sub>2</sub> SO <sub>4</sub>	120.9 $\mu\text{g h}^{-1} \text{mg}_{\text{cat}}^{-1}$ (-0.2 V vs. RHE)	29.6	11
BCN nanosheets	0.1 M HCl	7.75 $\mu\text{g h}^{-1} \text{mg}_{\text{cat}}^{-1}$ (-0.3 V vs. RHE)	13.79	12
SA-Mo/NPC	0.1 M KOH	34.0 $\pm$ 3.6 $\mu\text{g h}^{-1} \text{mg}_{\text{cat}}^{-1}$ (-0.3 V vs. RHE)	14.6 $\pm$ 1.6	13
PCN	0.1 M HCl	8.09 $\mu\text{g h}^{-1} \text{mg}_{\text{cat}}^{-1}$ (-0.2 V vs. RHE)	11.05	14
Fe <sub>SA</sub> -N-C	0.1 M KOH	7.48 $\mu\text{g h}^{-1} \text{mg}_{\text{cat}}^{-1}$ (0.0 V vs. RHE)	56.55	15

FL-BP NSs	0.01M HCl	31.37 $\mu\text{g h}^{-1} \text{mg}^{-1}$ (-0.7 V vs. RHE)	5.07 (-0.6 V vs. RHE)	16
BP@SnO <sub>2-x</sub> nanotube	0.1M Na <sub>2</sub> SO <sub>4</sub>	48.87 $\mu\text{g h}^{-1} \text{mg}^{-1}$ (-0.4 V vs. RHE)	14.6	17
Fe <sub>3</sub> O <sub>4</sub> /Ti	0.1 M Na <sub>2</sub> SO <sub>4</sub>	12.51 $\mu\text{g h}^{-1} \text{mg}^{-1}$ (-0.4 V vs. RHE)	2.6	18
Mn <sub>3</sub> O <sub>4</sub> nanocubes	0.1 M Na <sub>2</sub> SO <sub>4</sub>	11.6 $\mu\text{g h}^{-1} \text{mg}^{-1}_{\text{cat}}$ (-0.8 V vs. RHE)	3.0	19
Zr-TiO <sub>2</sub>	0.1 M KOH	8.9 $\mu\text{g h}^{-1} \text{mg}^{-1}_{\text{cat}}$ (-0.45 V vs. Ag/AgCl)	17.3	20
Fe-TiO <sub>2</sub>	0.5 M LiClO <sub>4</sub>	25.47 $\mu\text{g h}^{-1} \text{mg}^{-1}_{\text{cat}}$ (-0.40 V vs. RHE)	25.6	21
NiO/G	0.1 M Na <sub>2</sub> SO <sub>4</sub>	18.6 $\mu\text{g h}^{-1} \text{mg}^{-1}_{\text{cat}}$ (-0.7 V vs. RHE)	7.8	22
Vo-WO <sub>3</sub>	HCl (pH=1)	4.2 $\mu\text{g h}^{-1} \text{mg}^{-1}_{\text{cat}}$ (-0.12 V vs. RHE)	6.8	23
S-rich MoS <sub>2</sub> nanosheets	0.1 M Li <sub>2</sub> SO <sub>4</sub>	43.4 $\mu\text{g h}^{-1} \text{mg}^{-1}_{\text{cat}}$ (-0.45 V vs. RHE)	9.81	24
Fe <sub>3</sub> S <sub>4</sub> nanosheets	0.1 M HCl	75.4 $\mu\text{g h}^{-1} \text{mg}^{-1}_{\text{cat}}$ (-0.4 V vs. RHE)	6.45	25
CoP/CNs	0.1M Na <sub>2</sub> SO <sub>4</sub>	48.9 $\mu\text{g h}^{-1} \text{mg}^{-1}$ (-0.4 V vs. RHE)	8.7	26
VN NPs	0.05M H <sub>2</sub> SO <sub>4</sub>	40.392 $\mu\text{g h}^{-1} \text{mg}^{-1}$ (-0.1 V vs. RHE)	6.0	27
NPC-500	0.005 M H <sub>2</sub> SO <sub>4</sub>	22.3 $\mu\text{g h}^{-1} \text{mg}^{-1}$ (-0.4 V vs. RHE)	9.98	28
B4C nanosheet	0.1 M HCl	26.57 $\mu\text{g h}^{-1} \text{mg}^{-1}_{\text{cat}}$ (-0.75 V vs. RHE)	15.95	29

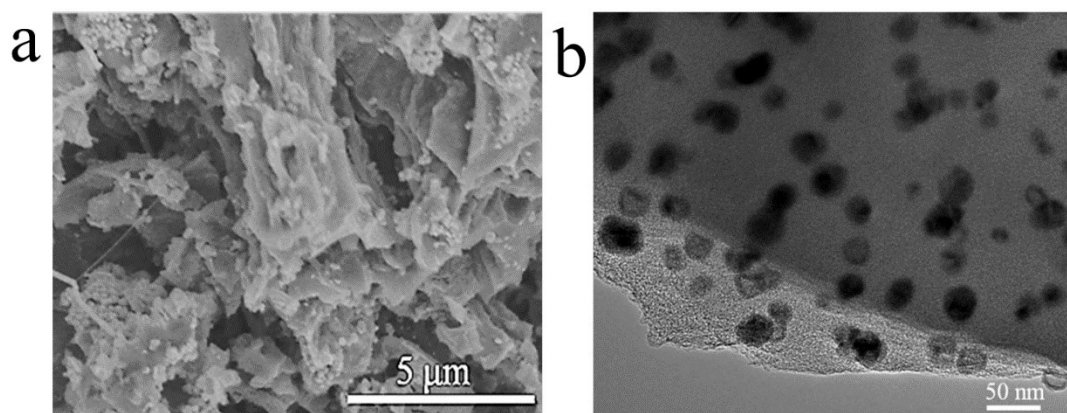


**Fig. S1** (a) SEM image and (b) TEM image of Cu NPs/CCG

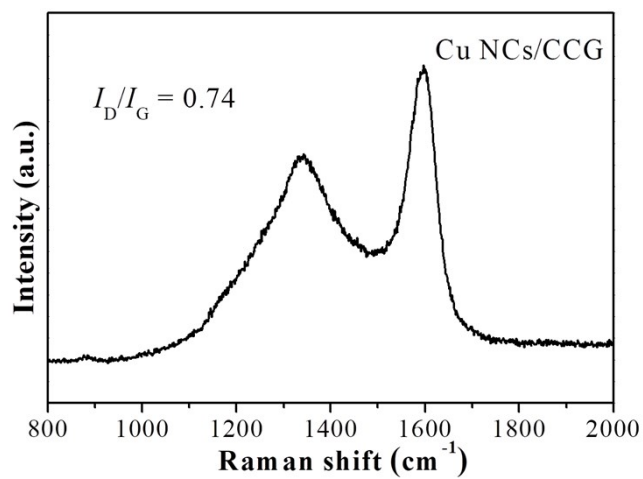


**Fig. S2** Raman spectrum of Cu NCs/CCG.

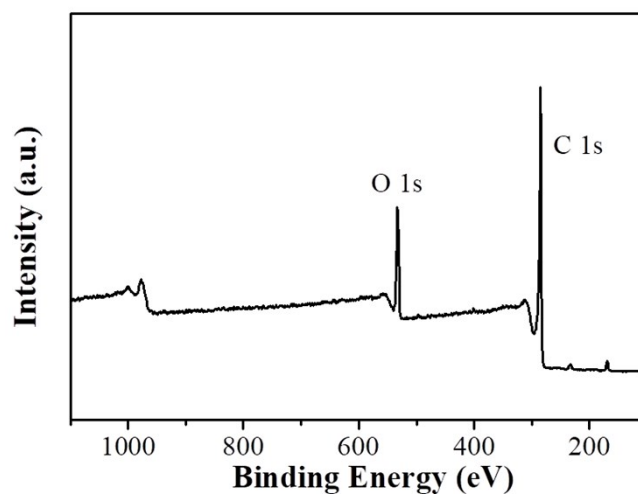


**Fig. S3** The surface survey XPS spectrum of the Cu NCs/CCG.

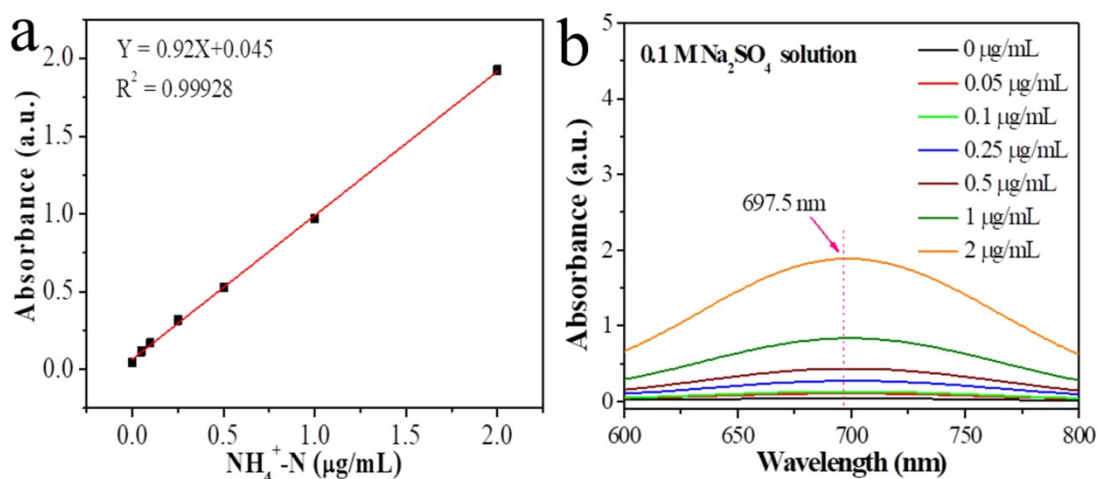


**Fig. S4** (a) The calibration curve used for calculation of  $\text{NH}_4^+\text{-N}$  concentration. (b) UV-Vis absorbance spectrum of the indophenol blue indicator with various concentrations of  $\text{NH}_4^+\text{-N}$  (0, 0.05, 0.1, 0.25, 0.5, 1, 2  $\mu\text{g/mL}$ ) after incubating for 1 h at room temperature.

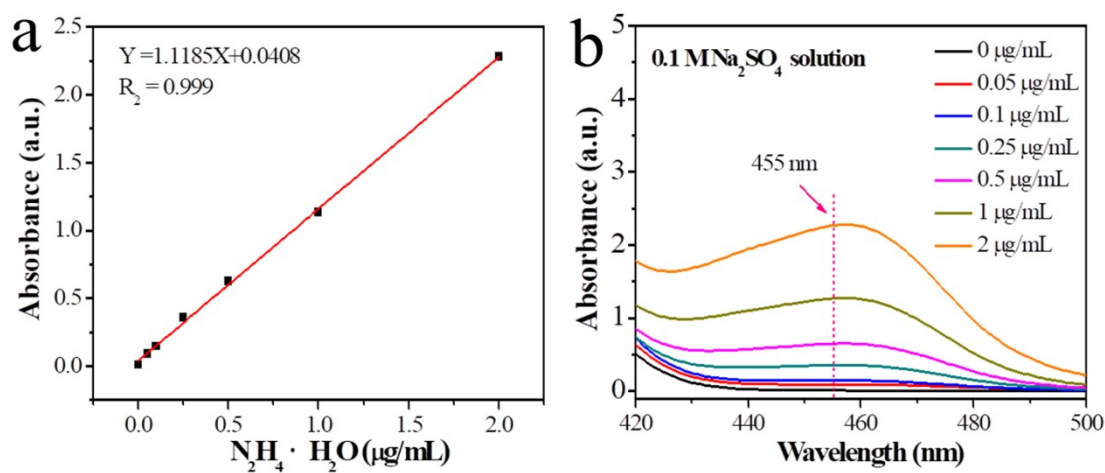


**Fig. S5** (a) UV-Vis absorption spectra with various concentrations of  $\text{N}_2\text{H}_4\cdot\text{H}_2\text{O}$  (0, 0.05, 0.1, 0.25, 0.5, 1.0, 2.0  $\mu\text{g/mL}$ ) after incubated for 20 min at room temperature. (b) The calibration curve used for calculation of  $\text{N}_2\text{H}_4\cdot\text{H}_2\text{O}$  concentrations.

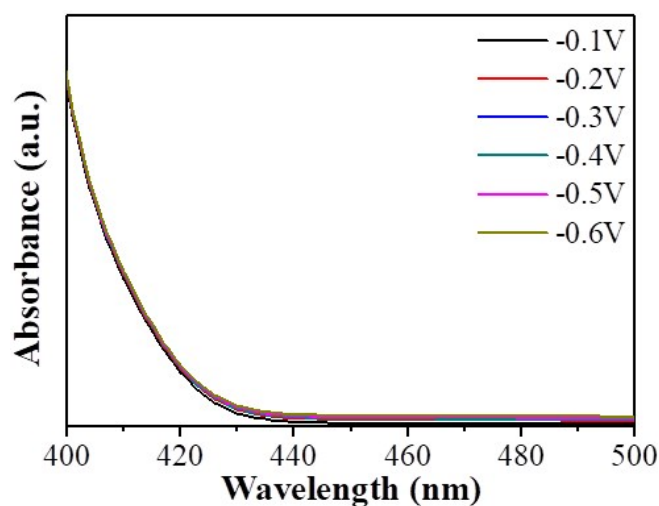


**Fig. S6** The  $\text{N}_2\text{H}_4\cdot\text{H}_2\text{O}$  UV-Vis absorption spectra of samples after ENRR measurement at different potentials in 0.1 M  $\text{Na}_2\text{SO}_4$  electrolyte.

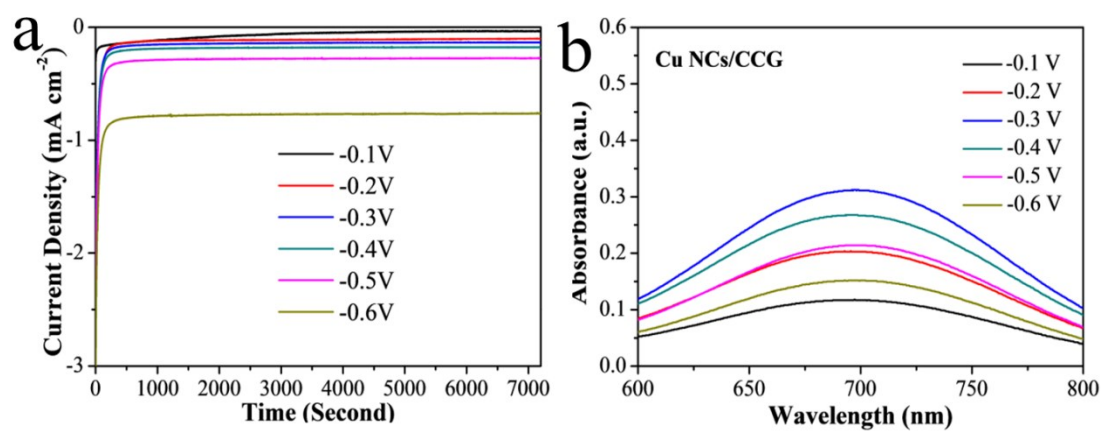


**Fig. S7** (a) Time-dependent current density curves of Cu NCs/CCG at different potentials in 0.1 M  $\text{Na}_2\text{SO}_4$  electrolyte and (b) corresponding UV-Vis absorption spectra of electrolytes colored with indophenols indicator after electrolysis at different potentials for 2h.

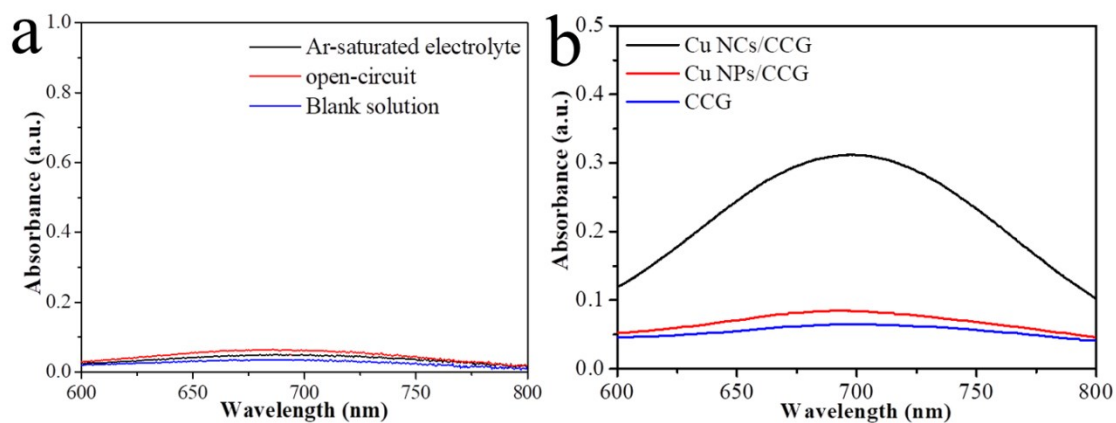


**Fig. S8** (a) UV-Vis absorption spectra of samples after ENRR reaction in 0.1 M  $\text{Na}_2\text{SO}_4$  electrolyte. (b) UV-Vis absorption spectra of CCG, Cu NPs/CCG and Cu NCs/CCG after ENRR reaction at  $-0.3\text{V}$ (vs. RHE) in 0.1 M  $\text{Na}_2\text{SO}_4$  electrolyte.

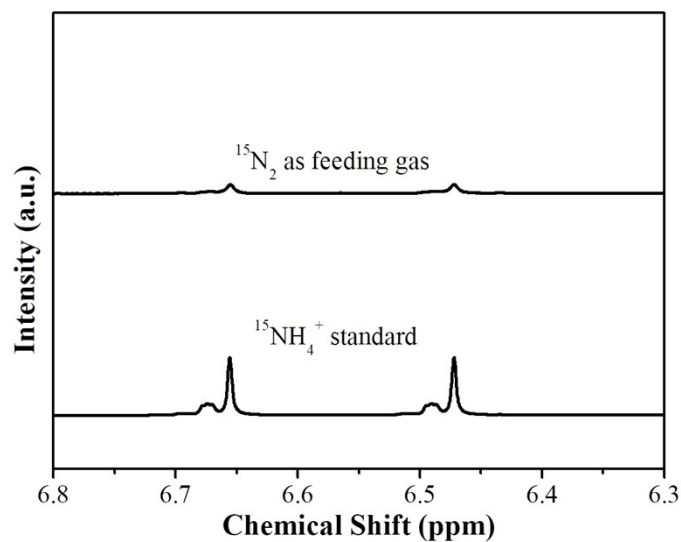


**Fig. S9** The  $^1\text{H}$  NMR spectra of the NRR sample using  $^{15}\text{N}_2$  as the feeding gas and  $^{15}\text{NH}_4^+$  standard.

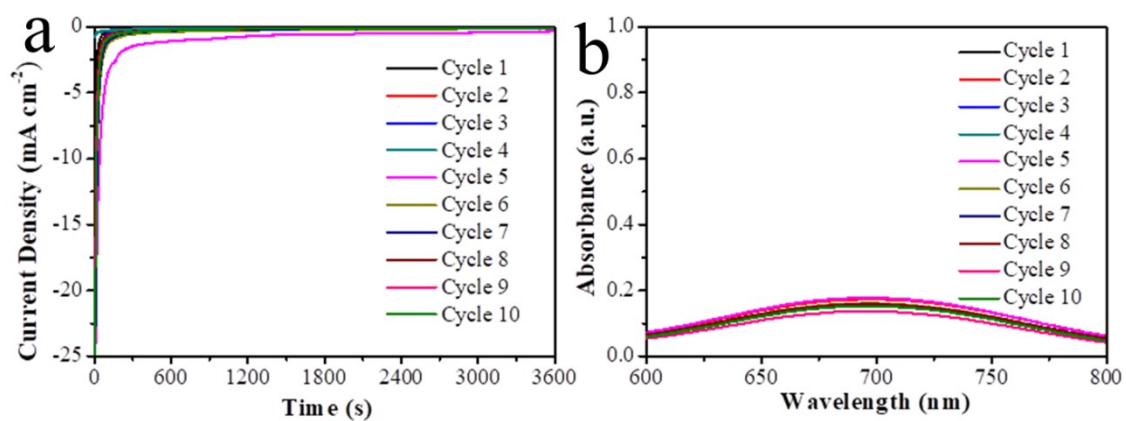


**Fig. S10** (a) Time-dependent current density curves and (b) UV-Vis absorption spectra of the different cycle numbers of Cu NCs/CCG in 0.1 M Na<sub>2</sub>SO<sub>4</sub> electrolyte for 1 h.

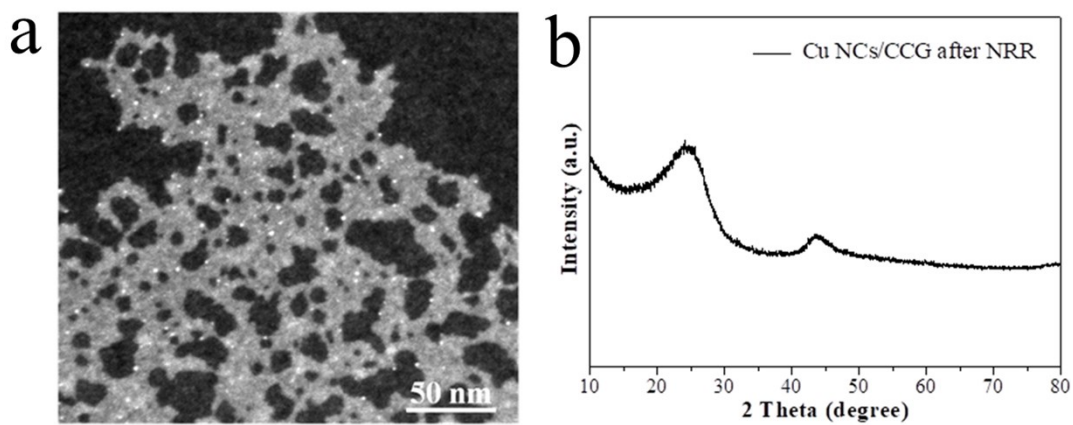


**Fig. S11** (a) XRD patterns and (b) HADDF-STEM image of Cu NCs/CCG catalyst after durability test.

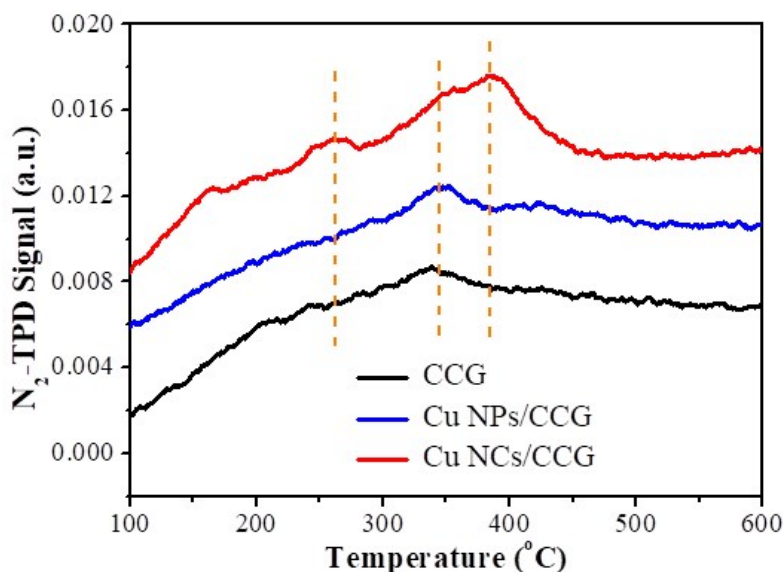


**Fig. S12** The N<sub>2</sub>-TPD profiles of CCG, Cu NPs/CCG and Cu NCs/CCG.

## References

1. S. Zhang, C. Zhao, Y. Liu, W. Li, J. Wang, G. Wang, Y. Zhang, H. Zhang and H. Zhao, *Chem. Commun*, 2019, **55**, 2952-2955.
2. F. Wang, Y. P. Liu, H. Zhang and K. Chu, *Chem Cat Chem*, 2019, **11**, 1–8.
3. S. Zhang, W. Li, Y. Liu, J. Wang, G. Wang, Y. Zhang, M. Han and H. Zhang, *Inorg. Chem. Front*, 2019, **6**, 2832-2836.
4. Y. X. Lin, S. N. Zhang, Z. H. Xue, J. J. Zhang, H. Su, T. J. Zhao, G. Y. Zhai, X.H. Li, M. Antonietti and J.S. Chen, *Nat. Commun*, 2019, **10**, 4380.
5. W. Zang, T. Yang, H. Zou, S. Xi, H. Zhang, X. Liu, Z. Kou, Y. Du, Y. P. Feng, L. Shen, L. Duan, J. Wang and S. J. Pennycook, *ACS Catal*, 2019, **9**, 10166-10173.
6. X. Guo, W. Yi, F. Qu and L. Lu, *J. Power Sources*, 2019, **448**, 227417.
7. H. Yu, Z. Wang, D. Yang, X. Qian, Y. Xu, X. Li, H. Wang and L. Wang, *J. Mater. Chem. A*, 2019, **7**, 12526-12531.
8. X. Huang, *Angew. Chem., Int. Ed.*, 2019, DOI:10.1002/anie.201913122.
9. M. M. Shi, D. Bao, B. R. Wulan, Y. H. Li, Y. F. Zhang, J. M. Yan and Q. Jiang, *Adv. Mater*, 2017, **29**, 1606550.
10. D. Bao, Q. Zhang, F. L. Meng, H. X. Zhong, M. M. Shi, Y. Zhang, J. M. Yan, Q. Jiang and X. B. Zhang, *Adv. Mater.*, 2017, **29**, 1604799.
11. Z. Geng, Y. Liu, X. Kong, P. Li, K. Li, Z. Liu, J. Du, M. Shu, R. Si and J. Zeng, *Adv. Mater.*, 2018, **30**, 1803498.
12. C. Chen, D. Yan, Y. Wang, Y. Zhou, Y. Zou, Y. Li and S. Wang, *Small Methods*, 2019, **15**, 1805029.
13. L. Han, X. Liu, J. Chen, R. Lin, H. Liu, F. Lü, S. Bak, Z. Liang, S. Zhao, E. Stavitski, J. Luo, R. R. Adzic and H. L. Xin, *Angew. Chem., Int. Ed*, 2019, **58**, 2321-2325.

14. C. Lv, Y. Qian, C. Yan, Y. Ding, Y. Liu, G. Chen and G. Yu, *Angew. Chem., Int. Ed.*, 2018, **57**, 10246-10250.
15. M. Wang, S. Liu, T. Qian, J. Liu, J. Zhou, H. Ji, J. Xiong, J. Zhong and C. Yan, *Nat. Commun*, 2019, **10**, 341.
16. L. Zhang, L. X. Ding, G.-F. Chen, X. Yang and H. Wang, *Angew. Chem., Int. Ed.*, 2019, **58**, 2612-2616.
17. Y. T. Liu, D. Li, J. Yu and B. Ding, *Angew. Chem., Int. Ed.*, 2019, **58**, 16439-16444.
18. Q. Liu, X. Zhang, B. Zhang, Y. Luo, G. Cui, F. Xie and X. Sun, *Nanoscale*, 2018, **10**, 14386-14389.
19. X. Wu, L. Xia, Y. Wang, W. Lu, Q. Liu, X. Shi and X. Sun, *Small Methods*, 2018, **14**, 1803111.
20. N. Cao, Z. Chen, K. Zang, J. Xu, J. Zhong, J. Luo, X. Xu and G. Zheng, *Nat. Commun.*, 2019, **10**, 2877.
21. T. Wu, X. Zhu, Z. Xing, S. Mou, C. Li, Y. Qiao, Q. Liu, Y. Luo, X. Shi, Y. Zhang, X. Sun, *Angew. Chem. Int. Ed.* 2019, **58**, 18449.
22. K. Chu, Y. P. Liu, J. Wang and H. Zhang, *ACS Appl. Energy Mater.*, 2019, **2**, 2288-2295.
23. Z. Sun, R. Huo, C. Choi, S. Hong, T. S. Wu, J. Qiu, C. Yan, Z. Han, Y. Liu, Y.-L. Soo and Y. Jung, *Nano Energy*, 2019, **62**, 869-875.
24. Y. Liu, M. Han, Q. Xiong, S. Zhang, C. Zhao, W. Gong, G. Wang, H. Zhang and H. Zhao, *Adv. Energy Mater.*, 2019, **9**, 1803935.
25. X. Zhao, X. Lan, D. Yu, H. Fu, Z. Liu and T. Mu, *Chem. Commun.*, 2018, **54**, 13010-13013.
26. S. Zhang, W. Gong, Y. Lv, H. Wang, M. Han, G. Wang, T. Shi and H. Zhang, *Chem. Commun*, 2019, **55**, 12376-12379.
27. X. Yang, J. Nash, J. Anibal, M. Dunwell, S. Kattel, E. Stavitski, K. Attenkofer, J. G. Chen, Y. Yan and B. Xu, *J. Am. Chem. Soc.*, 2018, **140**, 13387-13391.
28. C. Zhao, S. Zhang, M. Han, X. Zhang, Y. Liu, W. Li, C. Chen, G. Wang, H. Zhang and H. Zhao, *ACS Energy Lett.*, 2019, **4**, 377-383.
29. W. Qiu, X.-Y. Xie, J. Qiu, W.-H. Fang, R. Liang, X. Ren, X. Ji, G. Cui, A. M. Asiri, G. Cui, B. Tang and X. Sun, *Nat. Commun*, 2018, **9**, 3485.